Glassy carbon electrode modified with 7,7,8,8-tetracyanoquinodimethane and graphene oxide triggered a synergistic effect: low-potential amperometric detection of reduced glutathione.

YUAN, B., XU, C., ZHANG, R., LV, D., LI, S., ZHANG, D., LIU, L. and FERNANDEZ, C.

2017

Glassy carbon electrode modified with 7,7,8,8-tetracyanoquinodimethane and graphene oxide triggered a synergistic effect：low-potential amperometric detection of reduced glutathione

Baiqing Yuan [a, *], Chunying Xu [a], Renchun Zhang [a], Donghui Lv [a], Sujuan Li [a], Daojun Zhang [a], Lin Liu [a], Carlos Fernandez [b, *]

[a] Henan Province Key Laboratory of New Optoelectronic Functional Materials, College of Chemistry and Chemical Engineering, Anyang Normal University, Anyang 455000, Henan, China

[b] School of Pharmacy and Life Sciences, Robert Gordon University, Garthdee Road, Aberdeen AB10 7GJ, United Kingdom.

*** Corresponding author.**

E-mail: baiqingyuan1981@126.com (B. Yuan); c.fernandez@rgu.ac.uk (C. Fernandez)

Abstract

A sensitive electrochemical sensor based on the synergistic effect of 7,7,8,8-tetracyanoquinodimethane (TCNQ) and graphene oxide (GO) for low-potential amperometric detection of reduced glutathione (GSH) in pH 7.2 phosphate buffer solution (PBS) has been reported. This is the first time that the combination of GO and TCNQ have been successfully employed to construct an electrochemical sensor for the detection of glutathione. The surface of the glassy carbon electrode (GCE) was modified by a drop casting using TCNQ and GO. Cyclic voltammetric measurements showed that TCNQ and GO triggered a synergistic effect and exhibited an unexpected electrocatalytic activity towards GSH oxidation, compared to GCE modified with only GO, TCNQ or TCNQ/electrochemically reduced GO. Three oxidation waves for GSH were found at -0.05, 0.1 and 0.5 V, respectively. Amperometric techniques were employed to detect GSH sensitively using a GCE modified with TCNQ/GO at -0.05 V. The electrochemical sensor showed a wide linear range from 0.25 to 124.3 μM and 124.3 μM to 1.67 mM with a limit of detection of 0.15 μM. The electroanalytical sensor was successfully applied towards the detection of GSH in an eye drop solution.

Keywords: Electrochemical sensor; 7,7,8,8-tetracyanoquinodimethane (TCNQ); Graphene oxide; reduced glutathione

1. Introduction

Glutathione (GSH, γ-glutamyl-L-cysteinyl-glycine), the most abundant tripeptide thiol in eukaryotic and mammalian cells, performs a high number of physiological roles including protection against natrosative and oxidative stress (Areias et al., 2016). GSH has been found in both mammalian and plant tissue over the concentration range from 1 to 10 mM (Valero-Ruiz et al., 2016), and its levels are an indicator of various diseases such as HIV, cancer, Alzheimer's disease, and diabetes (Harfield et al., 2012). Therefore, developing sensitive and selective methods for GSH detection has attracted a lot of attention for medical diagnosis.

Electrochemcal determication of GSH is gaining momentum among other analytical methods due to its simplicity, high sensitivity, low cost and fast analysis (Harfield et al., 2012). The electrochemical oxidation of GSH at bare GCE requires high overpotential. As a result, various electrocatalysts have been utilized either modified on the electrode surface or placed in solution as a mediator to decrease the overpotential of GSH. The reported modification materials and mediators found in literature are thoroughly reviewed in **Table 1**. The electrochemical techniques most commonly employed are differential pulse voltammetry (DPV) and amperometric detection. However, a key problem with the analysis of GSH utilizing DPV is that the voltammetric peak resulting from the electrochemical oxidation of GSH may overlap with the electroactive coexisting species such as ascobic acid (AA), uric acid (UA), dopamine (DA) and cysteine (CYS). When amperometric detection is employed, the oxidation potential of GSH is required to be much lower than these coexisting species

to prevent their interference.

7,7,8,8-Tetracyanoquinodimethane (TCNQ) is an effective electron transfer mediator due to the presence of four cyano groups and π conjugation bonds, which can form organic charge-transfer complexes and ion-radical salts such as K (TCNQ) and Na (TCNQ) (Zamfir, et al., 2013; Paczosa-Bator et al., 2015). In addition, TCNQ has attracted considerable interest in the fabrication of electrochemical sensors for carbamate drugs (Zamfir, et al., 2013), K^+ (Paczosa-Bator et al., 2015), acetylcholinesterase inhibitors (Rotariu et al., 2012) and ascobic acid (Murthy and Anita, 1994). GO is a highly oxidized derivative of graphene, which possesses a large amount of oxygen functional groups such as hydroxyl, epoxide, carboxyl, and carbonyl groups (Zhu et al., 2010). The oxygen functional groups can increase the charge transfer resistance, but play an essential role in the electrocatalytic oxidation of some small molecules including AA (Uhma et al., 2011), DA (Xiong and Jin, 2011), dihydroxybenzene isomers, and L-methionine (Zhang et al., 2014). To the best of our knowledge, we have reported for the first time the fabrication of an electrochemical sensor using GCE modified with TCNQ and GO for the detection of GSH. In addition, the modified GCE sensor with TCNQ/GO showed an unexpected electrocatalytic activity towards GSH oxidation at a low potential compared to electrodes modified with only GO, TCNQ and TCNQ/electrochemically reduced GO (rGO). Furthermore, TCNQ and GO also showed a synergistic effect on the electrocatalytic oxidation of GSH with the oxidation overpotential decreasing greatly. Finally, based on the TCNQ/GO/GCE electrode, sensitive amperometric determination of GSH was

successfully achieved.

2. Experimental

2.1. Chemicals and solutions

TCNQ, GSH, CYS, DA, AA, and UA were purchased from Sigma-Aldrich. GO was acquired from Nanjing XFNano Materials Tech Co., Ltd. All other chemicals were of analytical reagent grade, and doubly distilled water was used to prepare all the solutions. 0.1 M phosphate buffer solution (PBS, pH 7.2) was employed as the background electrolyte.

2.2. Apparatus

Scanning electron microscopy (SEM) images were obtained with a Hitachi SU8010 (Japan) scanning electron microscope. A CHI 842C electrochemical workstation (Austin, TX, USA) was used to perform all the electrochemical experiments with a conventional three-electrode system, which included a GCE as the working electrode, a platinum coil as an auxiliary electrode, and an Ag/AgCl (saturated KCl) as the reference electrode.

2.3. Electrode preparation and modification

Prior to each experiment, GCE with a geometric area of 0.07 cm^2 was polished with 1, 0.3, and 0.05 μm alumina paste to a mirror finish, subsequently, the electrode was rinsed with water, and finally an ultrasonic treatment in water and ethanol was applied, respectively. GO modified GCE was prepared by droping a 5 μL of 1 mg/mL GO aqueous solution on the cleaned electrode and kept to dry at room temperature. Due to the low surface tension of acetone solution, TCNQ modified electrodes were prepared

by a drop casting method via solvent evaporation (Nafady et al., 2006). Briefly, the GO modified GCE or bare GCE was dipped in a 10 mM fresh solution of TCNQ in acetone for one minute and then kept in air to dry face down. To fabricate rGO modified GCE, firstly, the GO/GCE was electrochemically reduced in pH 4.0 acetate buffer by amperometric method for 500 s at -1.2 V, then the electrode was modified with TCNQ using the similar method as TCNQ/GO/GCE. The electroactive surface areas of these electrodes could be calculated by the Randles–Sevcik equation (Supplementary information).

3. Results and discussion

3.1. SEM Characterization of TCNQ modified electrodes

The electrode surface characterization was analyzed by SEM. **Fig. 1** shows the SEM images of TCNQ modified electrode by a drop casting method. As shown in **Fig. 1D, E, and F**, irregular TCNQ plates erected on the surface of GCE without GO due to gravity. However, in the presence of GO, rhombic TCNQ plates structures were formed and lay on the surface of GO/GCE (**Fig. 1A, B, and C**), those structures formation were attributed to the π-π interaction between GO and TCNQ. The size of the formed TCNQ crystals were found to be over the range from 5 to 30 μm.

3.2. Electrochemical properties of TCNQ modified electrodes

Next, the electrochemical properties of TCNQ modified electrodes were investigated. TCNQ exhibits two electrochemically reversible one-electron waves, which were associated to the generation of $TCNQ^{\cdot -}$ and $TCNQ^{2-}$ by using the following equations:

133 $TCNQ + e^- = TCNQ^{\cdot -}$ (1)

134 $TCNQ^{\cdot -} + e^- = TCNQ^{2-}$ (2)

135 **Fig. 2A *Inset*** shows the CVs of TCNQ immobilized on GCE by a drop casting
136 method in 0.1 M pH 7.2 PBS. It can be seen that a pair of typical redox peaks
137 appeared at 0.5 and -0.15 V, respectively. Surface-immobilized TCNQ also undergoes
138 a remarkable 'inert zone' in which no faradaic reaction yields, suggesting a typical
139 solid-solid phase transformation in terms of nucleation and growth (Gómez and
140 Rodríguez-Amaro, 2006). Further, with the increasing cycle, the voltammetric peak
141 heights decay due to the dissolution of TCNQ into the solution (Bond et al., 1998).
142 The results obtained are in good agreement with previous reports (Gómez and
143 Rodríguez-Amaro, 2006; Bond et al., 1998). The electrochemical behaviour of
144 immobilized TCNQ on the surface of GO or rGO was also studied, as shown in **Fig.**
145 **2B and C *Inset***. Both CVs differ considerably from that obtained at TCNQ/GCE. The
146 electrochemical processes at the GCE modified with TCNQ/GO showed three pairs of
147 redox waves (**Fig. 2B *Inset***). According to Eqs. (1) and (2), the two corresponding
148 oxidation peak potentials were observed at -0.05 and 0.36 V, and the corresponding
149 reduction waves appeared at -0.15 and 0.10 V, respectively. The peak 3 showed in Fig.
150 2B Inset is due to the electrochemical behavior of the oxygen functional species on
151 GO, which can also be found in **Fig. 2D** (Yuan et al., 2013c; Ndamanisha et al., 2009)**.**
152 When the GCE was modified with TCNQ/rGO, two electrochemical processes were
153 identified and the corresponding oxidation and reduction waves changed to -0.17 and
154 0.13 V, and -0.32 and 0.05 V, respectively. In addition, the two electrochemical

processes became much more reversible than that obtained at TCNQ/GO/GCE. This was attributed to the fast electron transfer rate of rGO. The results also showed that the dissolution of TCNQ in solution decreased at the TCNQ/GO/GCE due to the π-π interaction between TCNQ and GO.

3.3. Electrocatalytic oxidation of GSH based on TCNQ modified electrodes

The electrochemical oxidation of GSH using various modified electrode surfaces in 0.1 M pH 7.2 PBS by cyclic voltammogram (CV) at a scan rate of 0.1 V/s was also investigated, as shown in **Fig. 2**. When the GCE was modified with GO an oxidation peak was observed at 0.22 V due to the GSH oxidation reaction to GSSG (**Fig. 2D**). This is caused by the electrocatalyic activity of oxygen functional species present on GO towards the oxidation of GSH. The oxidation peak of GSH appeared at 0.7 V when the GCE was modified with TCNQ (**Fig. 2A**). Upon addition of GSH to the solution, three oxidation waves emerged at the TCNQ/GO/GCE with the corresponding oxidation peak potentials of -0.05, 0.1, and 0.5 V, respectively shown in. **Fig. 2B**. These three enhanced oxidation waves were attributed to the electrocatalysis of $TCNQ^{\cdot -}$, oxygen functional groups, and $TCNQ^{2-}$ with the oxidation of GSH. In addition, the catalytic current at 0.1 V is much higher than that obtained at GO/GCE (**Fig. 2D**) with a much lower oxidation potential. The introduction of TCNQ enhanced the electrocatalytic activity of oxygen functional groups present on GO. However, there was no electrocatalytic current observed until 0.35 V when the GCE surface was modified with TCNQ/rGO, even though rGO has high electrical conductivity and fast electron transfer rate. The comparison results showed that

TCNQ and GO had a synergistic effect, which exhibited unexpected electrocatalytic activity towards the oxidation of GSH. The electrocatalytic mechanism proposed is shown by equations 3 and 4:

$$TCNQ^{\cdot -} + 2GSH = TCNQ + GSSG + 2H^{+} \quad (3)$$

$$TCNQ^{2-} + 2GSH = TCNQ + GSSG + 2H^{+} \quad (4)$$

The electrochemical detection of GSH in physiological samples had presented a major obstacle due to the presence of electroactive species such as AA, DA, UA, and CYS which often coexists with GSH. The ultra-low overpotential of GSH shown at the TCNQ/GO/GCE may overcome the interferences from these interfering species. Next, the selectivity of the proposed electrochemical sensor (modified GCE with TCNQ/GO) was investigated by CV. **Fig. 3** shows the CVs of TCNQ/GO/GCE in the absence (dotted line) and presence (solid line) of 0.2 mM AA (A), 5 mM CYS (B), 0.2 mM DA (C), and 0.2 mM UA (D) in 0.1 M 7.2 pH PBS at a scan rate of 0.1 V/s. The oxidation peak for UA was found to be at 0.38 V, which is much higher than the first and second oxidation wave of GSH because of the ultra-low overpotential of GSH at the TCNQ/GO/GCE. Two pairs of redox peaks were observed for DA. Further experiments indicated that the first oxidation process for DA at 0.23 V is essential to form the second oxidation. Therefore, the oxidation potential of DA is also higher than the first two oxidation waves of GSH. AA and CYS had a similar electrocatalytic oxidation as GSH, but the electrocatalytic current is lower than that of GSH. It was reported that the concentration of GSH in the cells can be up to 10 mM (Mesiter, 1988), while the basal level of AA in the extracellular fluid of the central nervous

system, is approximately 0.1 μM, and the physiological level of AA is about 0.1 mM (El-Said et al., 2010). Considering the far higher level of GSH compared to AA in physiological samples and high sensitivity for GSH detection of this method, the influence of AA may be decreased and even ignored by diluting the sample. In addition, AA can be removed from the sample by adding ascorbate oxidase (Silva, et al. 2013) before analysis. Therefore, it is possible to apply the mthod for the detection of GSH in biological fluids.

3.4. Amperometric sensing of GSH based on a GCE modified with TCNQ/GO

Next, we investigate the electrochemical detection of GSH on a GCE modified with TCNQ/GO using amperometric techniques. **Fig. 4** shows the amperometric response of TCNQ/GO/GCE to the successive additions of GSH in a stirring pH 7.2 PBS solution. Due to the high electrocatalytic activity of the TCNQ/GO/GCE towards the GSH oxidation, much lower potentials (-0.05 or 0.1 V) were used. For -0.05 V and 0.1 V amperometric sensing, the measured current increased with the GSH concentrations, and a linear response was observed over a concentration range of 0.25-124.3 μM (R^2=0.9928, *I*/μA=0.029+2.09 C/mM) and 124.3 μM-1.67 mM (R^2 =0.9989, *I*/μA=0.37+0.35 C/mM), and 0.25-174.3 μM (R^2=0.9956, I/μA=0.37+0.34 C/mM) and 174.3 μM-1.18 mM, (R^2=0.9972, I/μA=0.50+0.78 C/mM), respectively. The limit of detection was calculated to be 0.15 μM and 0.10 μM (S/N=3), respectively. The analytical performance of GSH with the GCE modified with TCNQ/GO reported in this work and other modified materials and mediators found in literature are thoroughly reviewed in **Table 1**. The oxidation potential of GSH at the

TCNQ/GO/GCE (-0.05 V) is much lower than those other materials or mediators but higher than catechol (-0.16 V) illustrated in Table 1. The TCNQ/GO/GCE also displayed a wide linear range for the detection of GSH compared to other electrodes. It should be noted that, with the addition of high GSH concentrations, the amperometric responses decreased with time, suggesting that further GSH oxidation was greatly hindered. This may be caused by the passivation of electrode due to the binding of the sulfur moiety to the electrode surface generated by the oxidation of GSH because the concentration of GSH reached a high level in the detection cell with the successive additions of GSH (Harfield, et al., 2012). The similar phenomenon was also reported in the previous literature (Yuan, et al., 2013c).

In order to assess the anti-interference performance of TCNQ/GO/GCE, the interference effect was also examined at the TCNQ/GO/GCE with 25 μM GSH in the presence of 4 μM AA, 4 μM CYS, 25 μM DA, and 25 μM UA by using amperometric technique (Supplementary information). The results showed that the presence of these electroactive species with the added concentration did not interfere with the determination of GSH due to the low detection potential at which was applied. This is also in agreement with the interference test by CV method in section 3.3.

The stability of the electrochemical sensor was investigated by a continuous operation and successive performance. After 2300 s of continuous operation of 25 μM GSH, 98% of its initial value was retained (Supplementary information). After being stored in air for one week and two weeks, respectively, the electrode had a 12% and 18% decrease in current response (Supplementary information). In addition, the RSD

was 4.7% for ten successive analysis of 25 μM GSH using the same electrode. This excellent stability of the presented sensor was due to the π-π interaction between GO and TCNQ.

3.5. Analysis of GSH in real samples

The applicability of the sensor was further evaluated by the analysis of GSH in an eye drop solution (purchased from Wuhan Wujing Medicine Co., Ltd, China). 2.0 μL sample without pretreatment was directly added to a stirring PBS solution at pH 7.2 (8.0 mL) for amperometric detection. The GSH concentration in the eye drops solution was found to be 60.8 mM, which is in agreement with the labeled value (65.0 mM). The recoveries were also estimated by adding GSH standards to the above solution. The results showed that the sensor gave the acceptable recoveries over the range between 94.7% and 106.1%.

4. Conclusions

A simple TCNQ and GO modified GCE was prepared and used for the electrocatalytic oxidation of GSH at physiological pH. The results showed that TCNQ and GO triggered an outstanding synergistic effect which enhanced the electrocatalytic activity towards the oxidation of GSH. As a result, the oxidation potential of GSH decreased to an ultra-low value (-0.05 V). Based on the TCNQ and GO modified GCE, low potential amperometric detection of GSH was achieved with wide linear range and low detection limit. The electrochemical protocol was successfully applied towards the detection of GSH in a real sample (eye drop solution) with a recovery from 94.7 to 106.1%. As an effective electrocatalysts, the TCNQ and

GO opens a new potential application in biosensing.

Acknowledgments

The authors would like to express their gratitude to the National Science Foundation of China (No. 21405005), the Joint Fund for Fostering Talents of National Natural Science Foundation of China and Henan Province (No. U1404208), the Program for Science and Technology Innovation Talents at the University of Henan Province (17HASTIT001), and the Scientific Research Foundation for Returned Overseas Chinese Scholars of State Education Ministry. CF would also like to express his gratitude to RGU for its support.

References

Areias, M.C.C., Shimizu, K., Compton, R.G., 2016. Analyst 141, 2904–2910.

Atta, N.F., Galal, A., Azab, S.M., 2012. Anal. Bioanal. Chem. 404, 1661–1672.

Bond, A.M. Fletcher, S., Symons, P.G., 1998. Analyst 123, 1891–1904.

Chatraei, F., Zare, H.R., 2011. Analyst 136, 4595–4602.

Chee, S.Y., Flegel, M., Pumera, M., 2011. Electrochem. Commun. 13, 963–965.

El-Said, W.A., Lee, J.H., Oh, B.K., Choi, J.W., 2010. Electrochem. Commun. 12, 1756–1759.

Ensafi, A.A. Karimi-Malehb, H. Mallakpour, S., 2013. Colloids Surf. B 104, 186–193.

Eremenko, A.V., Dontsova, E.A., Nazarov, A.P., Evtushenko, E.G., Amitonov, S.V., Savilov, S.V., Martynova, L.F., Lunin, V.V., Kurochkin, I.N., 2012. Electroanal. 24, 573–580.

Gómez, L., Rodríguez-Amaro, R., 2006. Langmuir 22, 7431–7436.

Harfield, J.C., Batchelor-McAuley, C., Compton, R.G., 2012. Analyst 137, 2285–2296.

He, H., Du, J., Hu, Y., Ru, J., Lu, X., 2013. Talanta 115, 381–385.

Hosseini, H., Ahmar, H., Dehghani, A., Bagheri, A., Tadjarodi, A., Fakhari, A.R., 2013. Biosens. Bioelectron. 42, 426–429.

Hou, Y., Ndamanisha, J.C., Guo, L., Peng, X., Bai, J., 2009. Electrochim. Acta 54, 6166–6171.

Huang, Y., Yan, H., Tong, Y., 2015. J. Electroanal. Chem. 743, 25–30.

Inoue, T., Kirchhoff, J.R., 2000. Anal. Chem. 72, 5755–5760.

309 Karimi-Maleh, H., Tahernejad-Javazmi, F., Ensafi, A., Moradi, R., Mallakpour, S.,
310 Beitollahi, H., 2014. Biosens. Bioelectron. 60, 1–7.
311 Lee, P.T., Goncalves, L.M., Compton, R.G., 2015. Sens. Actuators B: Chem. 221,
312 962–968.
313 Li, X., Zheng, L., Wang, Y., Zhang, N., Lou, Y. Xiao, T. Liu, J., 2015. RSC Adv. 5,
314 71749–71755.
315 Liu, B., Wang, M., Xiao, B., 2015. J. Electroanal. Chem. 757, 198–202.
316 Luz, R.C.S., Damos, F.S., Tanaka, A.A., Kubot, L.T., Gushikem, Y., 2008. Talanta 76,
317 1097–1104.
318 Medina-Ramos, J., Oyesanya, O., Alvarez, J.C., 2013. J. Phys. Chem. C 117,
319 902−912.
320 Mesiter, A., 1988. J. Bio. Chem. 263, 17205−17208.
321 Mu, S., Yang, Y., 2016. J. Electroanal. Chem. 780, 12–18.
322 Murthy, A.S.N., Anita, 1994. Biosens. Bioelectron. 9, 439–444
323 Narang, J., Chauhan, N., Jain, P., Pundir, C.S., 2012. Int. J. Biol. Macromol. 50,
324 672–678.
325 Ndamanisha, J.C., Bai, J., Qi, B., Guo L., 2009. Anal. Biochem. 386, 79–84.
326 Nafady, A., O'Mullane, A.P., Bond, A.M. Neufeld, A.K., 2006. Chem. Mater. 18,
327 4375–4384.
328 Oztekin, Y., Ramanaviciene, A., Ramanavicius, A., 2011. Electroanal. 23, 701–709.
329 Pacsial-Ong, E.J., McCarley, R.L., Wang, W., Strongin, R.M., 2006. Anal. Chem. 78,
330 7577–7581.

331 Paczosa-Bator, B., Pięk, M., Piech, R., 2015. Anal. Chem. 87, 1718–1725.
332 Pandey, P.C., Pandey, A.K., 2012. Analyst 137, 3306–3313.
333 Pang, H., Shi, Y., Du, J., Ma, Y., Li, G., Chen, J., Zhang, J., Zheng, H., Yuan, B.,
334 Electrochim. Acta 2012, 256–262.
335 Pereira-Rodrigues, N., Cofré, R., Zagal, J.H., Bedioui, Fethi., 2007. Bioelectrochem.
336 70, 147–154.
337 Raoof, J.B., Ojani, R., Baghayeri, M., 2009. Sens. Actuators B: Chem. 143, 261–269.
338 Rotariu, L., Zamfir, L.G., Bala, C., 2012. Anal. Chim. Acta 748, 81–88.
339 Safavi, A., Maleki, N., Farjami, E., Mahyari, F.A., 2009. Anal. Chem. 81, 7538–7543.
340 Salehzadeh, H., Nematollahi, D., 2013. Electrochim. Acta 111, 909– 915.
341 Shahmiria, M.R., Baharia, A., Karimi-Malehb, H., Hosseinzadehc, R., Mirnia, N.,
342 2013. Sens, Actuators B: Chem 177, 70–77.
343 Shayani-Jam, H., Nematollahi, D., 2010a. Chem. Commun. 46, 409–411.
344 Shayani-Jam, H., Nematollahi, D., 2011b. Electrochim. Acta 56, 9311–9316.
345 Silva, F.A.S., Silva, M.G.A., Lima, P.R., Meneghetti, M.R., Kubota, L.T., Goulart,
346 M.O.F., 2013. Biosens. Bioelectron. 50, 202–209.
347 Uhma, S., Tuyenb, N.H., Lee, J., 2011. Electrochem. Commun. 13, 677–680.
348 Valero-Ruiz, E., González-Sánchez, M.I. Batchelor-McAuley, C., Compton, R.G.,
349 2016. Analyst 141, 144–149.
350 Wang, X., Chen, X., Evans, D.G., Yang W., 2011. Sens. Actuators B: Chem. 160,
351 1444–1449.
352 Xiong, H., Jin, B., 2011. J. Electroanal.Chem. 661, 77–83.

Xu. H., Xiao, J., Liu, B., Griveau, S., Bedioui, F., 2015. Biosens. Bioelectron. 66,438–444

Yuan, B., Xu, C., Liu, L. Zhang, Q., Ji, S., Pi, L., Zhang, D., Huo, Q., 2013a. Electrochim. Acta 104, 78–83.

Yuan, B., Zhang, R., Jiao, X., Li, J., Shi, H., Zhang, D., 2014. Electrochem. Commun. 40, 92–95.

Yuan, B., Zeng, X., Deng, D., Xu, C., Liu, L., Zhang, J., Gao, Y., Pang, H., 2013b. Anal. Methods 5, 1779–1783.

Yuan, B., Zeng, X., Xu, C., Liu, L., Ma, Y., Zhang, D., Fan, Y., 2013c. Sens. Actuators B: Chem. 184, 15–20.

Zamfir, L.G., Rotariu, L., Bala, C., 2013. Biosens. Bioelectron. 46, 61–67.

Zhao, L., Zhao, L., Miao, Y., Zhang, C., 2016. Electrochim. Acta 206, 86–98.

Zhang, D., Xu, C., Li, S., Zhang, R., Yan, H., Miao, H., Fan, Y., Yuan, B., 2014. J. Electroanal. Chem. 717-718, 219–224.

Zhang, F., Wen, M., Cheng, M., Liu, D., Zhu, A., Tian, Y., 2010. Chem. Eur. J. 16, 11115–11120.

Zhu, Y., Murali, S., Cai, W.W., Li, X.S., Suk, J.W., Potts, J.R., Ruoff, R.S., 2010. Adv. Mater. 22, 3906–3924.

Figure captions

Fig. 1 SEM images of TCNQ/GO/GCE (A, B, and C) and TCNQ/GCE (D, E, and F) at different magnifications by a drop casting method.

Fig. 2 CVs of TCNQ/GCE (A), TCNQ/GO/GCE (B), TCNQ/rGO/GCE (C), and GO/GCE (D) in the presence (solid line, first cycle) and absence (dotted line, steady state cycle) of 5 mM GSH in 0.1 M 7.2 pH PBS at a scan rate of 0.1 V/s. *Inset* (A, B, C) first twenty cycles for corresponding electrodes.

Fig.3 CVs of TCNQ/GO/GCE in the absence (dotted line) and presence (solid line) of 0.2 mM AA (A), 5 mM CYS (B), 0.2 mM DA (C), and 0.2 mM UA (D) in 0.1 M 7.2 pH PBS at a scan rate of 0.1 V/s. *Inse*t is the CV of 5 mM GSH in the same condition.

Fig. 4 Amperometric detection of GSH by successive additions of GSH into a stirring pH 7.2 PBS solution at the TCNQ/GO/GCE at -0.05 (curve 1) and 0.1 V (curve 2). *Inset* (A): The corresponding calibration plot; (B): amplified response of the TCNQ/GO/GCE to lower concentration of GSH.

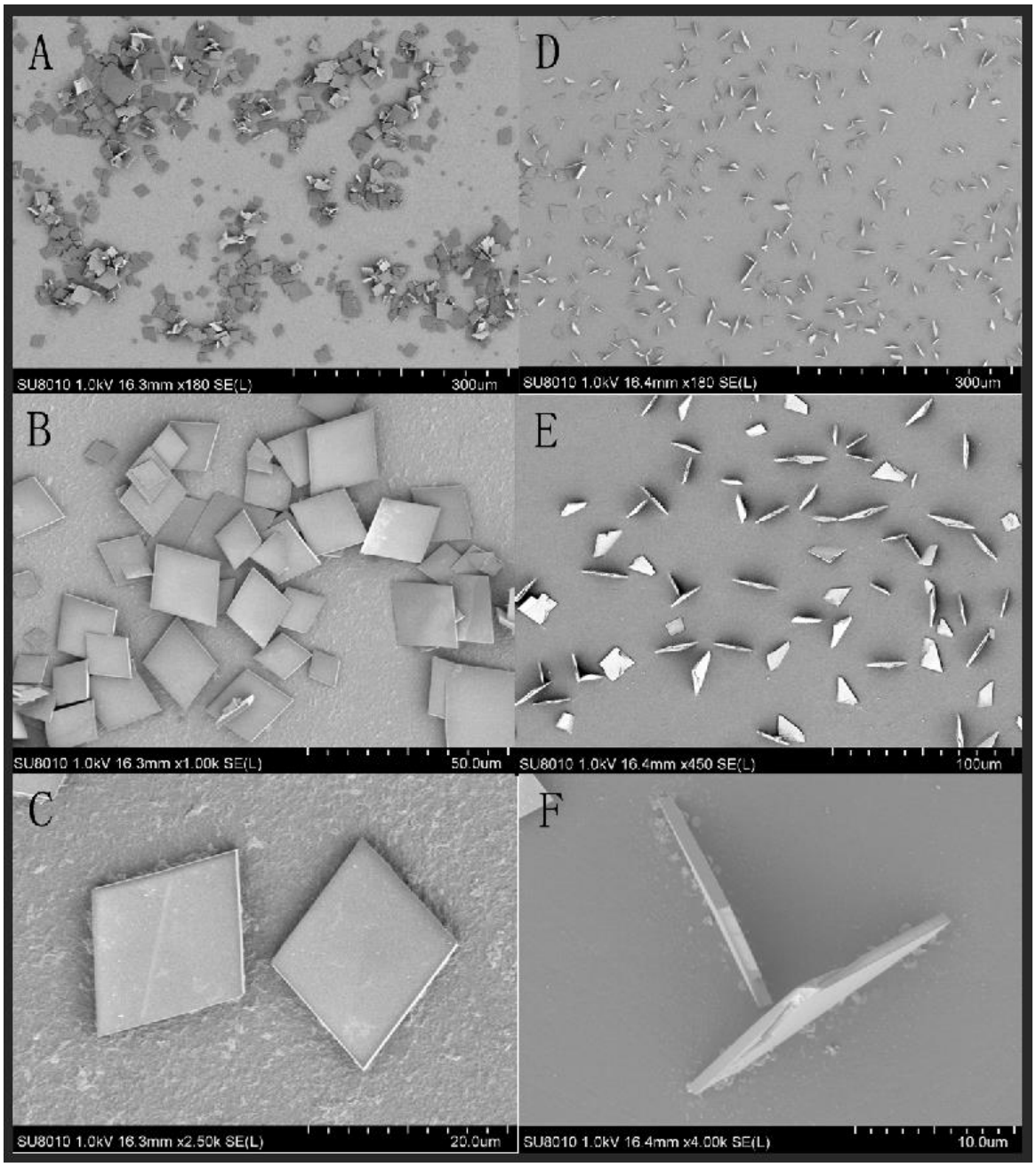

Figure 1. SEM images of TCNQ/GO/GCE (A, B, and C) and TCNQ/GCE (D, E, and F) at different magnifications by a drop casting method.

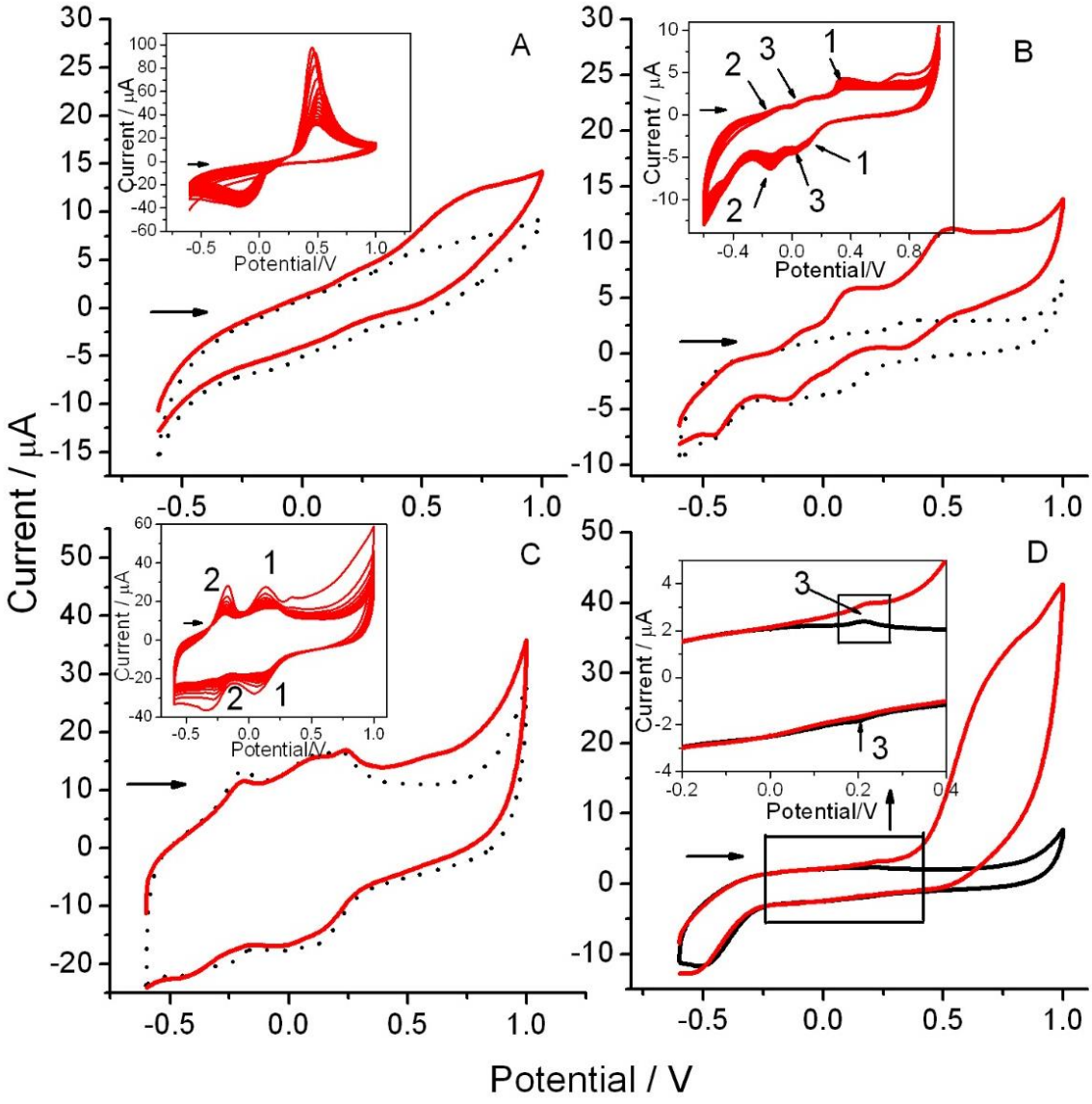

Figure 2. CVs of TCNQ/GCE (A), TCNQ/GO/GCE (B), TCNQ/rGO/GCE (C), and GO/GCE (D) in the presence (solid line, first cycle) and absence (dotted line, steady state cycle) of 5 mM GSH in 0.1 M 7.2 pH PBS at a scan rate of 0.1 V/s. *Inset* (A, B, C) first twenty cycles for corresponding electrodes.

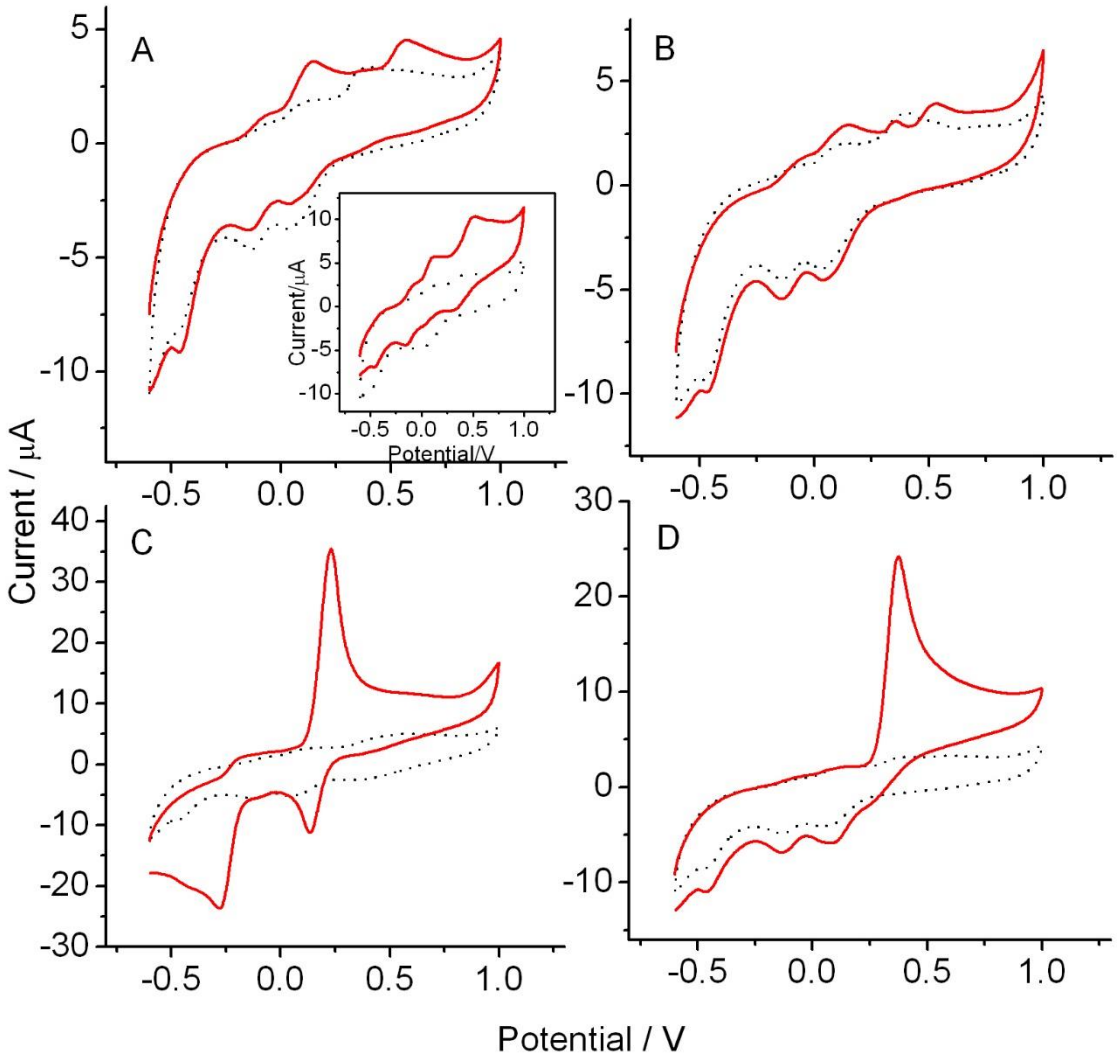

399

400 Figure 3. CVs of TCNQ/GO/GCE in the absence (dotted line) and presence (solid line) of 0.2 mM
401 AA (A), 5 mM CYS (B), 0.2 mM DA (C), and 0.2 mM UA (D) in 0.1 M 7.2 pH PBS at a scan rate
402 of 0.1 V/s. *Inset* is the CV of 5 mM GSH in the same condition.

403

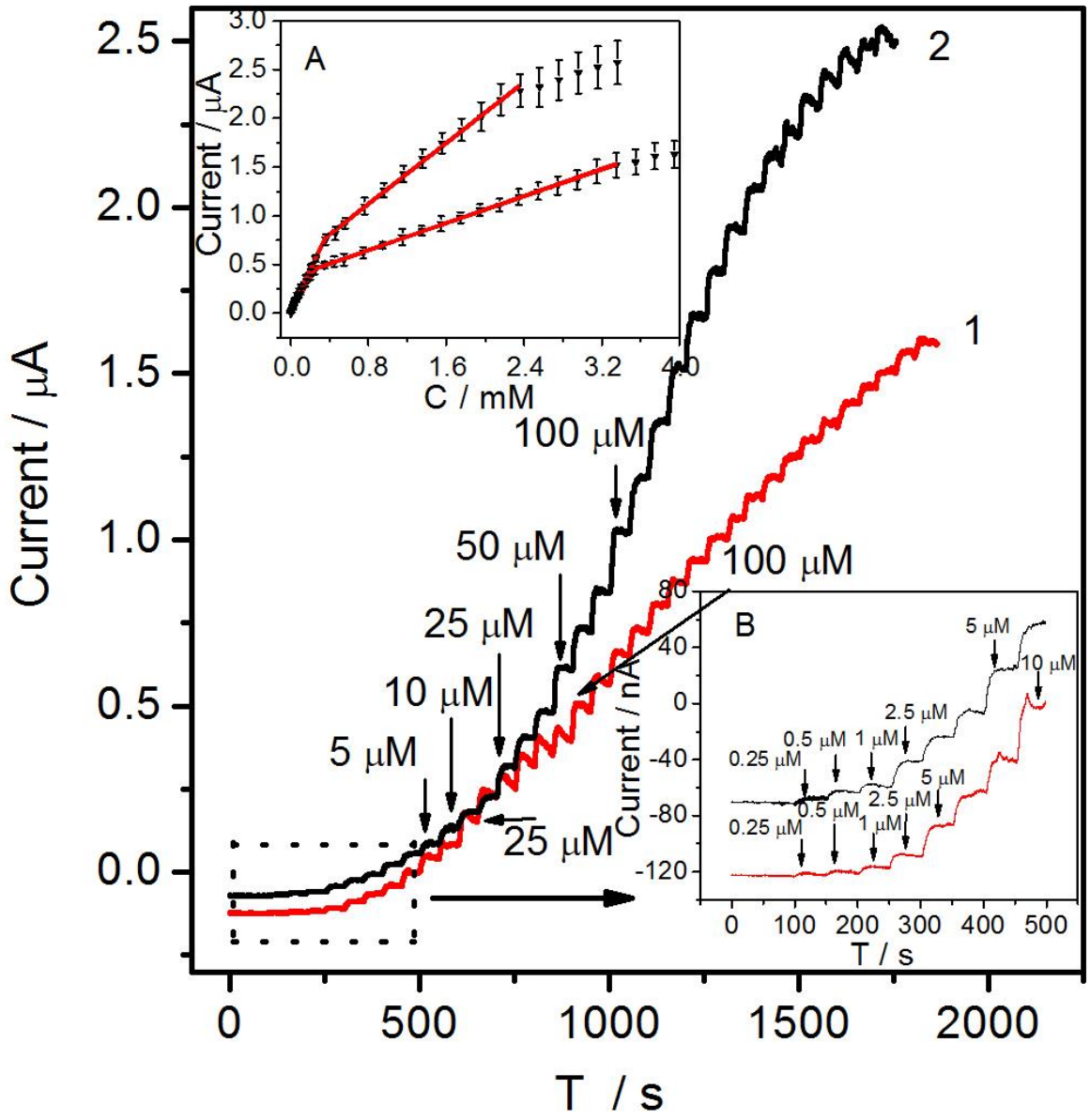

Figure 4. Amperometric detection of GSH by successive additions of GSH into a stirring pH 7.2 PBS solution at the TCNQ/GO/GCE at -0.05 (curve 1) and 0.1 V (curve 2). *Inset* (A): The corresponding calibration plot; (B): amplified response of the TCNQ/GO/GCE to lower concentration of GSH.

Table 1. Analytical performances for GSH detection based on various modification materials and mediators by different electrochemical methods.

Materials or mediators	Method	pH	OP/V	Linear range	LOD	References
NiO [Ml]	DPV	7.2	0.6 [a]	0.2 mM ~ 6.0 mM	0.2 mM	Chee et al., 2011

NiO microflower [Ml]	AMP	5.0	0.4 [a]	10 μM ~ 0.62 μM; 0.6 mM ~ 3.6 mM	10 μM	Pang et al., 2012
Electrodeposited NiO [Ml]	AMP	5.0	0.4 [a]	12.5 μM ~ 2.3 mM	2 μM	Yuan et al., 2013b
NiO_x/Cu_2O [Ml]	AMP	7.0	0.3 [a]	2 μM ~ 1.3 mM	0.3 μM	Yuan et al., 2013a
Poly-m-aminophenol [Ml]	AMP	4.0	0.5 [a]	0.1 μM ~ 5 μM	0.095 μM	Oztekin et al., 2011
CoPcTF [Ml]	AMP	7.4	0.18 [a]	1 μM ~ 818 μM	0.2 μM	Wang et al., 2011
CNT–SPE [Ml]	CV	7.0	0.4 [b]	10 μM ~ 100 μM	3 μM	Lee et al., 2015
MPT-HP-β-CD [Ml]	AMP	7.0	0.58 [a]	1 μM ~ 580 μM	0.87 μM	Li et al., 2015
Pd-IrO_2 [Ml]	AMP-CE	3.0	0.85 [a]	10 μM ~ 800 μM	2 μM	Xu et al., 2002
Electrochemical modified GO [Ml]	AMP	5.0	0.23 [a]	5 μM ~ 875 μM; 875 μM ~ 4.08 mM	5 μM	Yuan et al., 2013
Co-based metal-organic coordination polymer [Ml]	AMP	7.2	0.4 [a]	2.5 μM ~ 0.95 mM	2.5 μM	Yuan et al., 2014
NiHCF-gold [Ml]	LSV	4.0	0.65 [a]	1 μM ~1.4 mM	0.5 μM	Pandey and Pandey, 2012
Ag/CNT//polyaniline [Ml]	CV	6.0	0.4 [a]	0.3 μM ~ 3.5 mM	0.30 μM	Narang et al., 2012
Manganese dioxide [Ml]	AMP	7.5	0.45 [a]	0.5 μM ~ 10 μM	0.2 μM	Eremenko et al., 2012
Cobalt phthalocyanine [Ml]	CV	7.4	0.1 [c]	0.08 mM ~ 1 mM	~	Pereira-Rodrigues et al., 2006
Mesoporous carbon/CoO [Ml]	DPV	4.0	0.25 [a]	4 μM ~28 μM	~	Hou et al., 2009
Mesoporous carbon [Ml]	AMP	7.2	0.15 [a]	0.28 mM ~ 3 mM	~	Ndamanisha et

						al., 2009
Acetaminophen [Ml]	DPV	7.0	0.32 [c]	100 μM ~ 2.7 mM	0.37 μM	Chatraei and Zare, 2011
NiHCF/CTAB/AuNPs [Ml]	DPV	6.5	0.45 [a]	0.2 μM ~ 1 μM;	0.08 μM	He et al, 2013
Nanoscale Copper Hydroxide [Ml]	CV	7.2	0.15 [a]	1 μM ~ 50 μM; 0.1 mM ~ 1.8 mM	0.03 μM	Safavi et al., 2009
Nano-TiO_2/ferrocene carboxylic acid [Ml]	DPV	7.0	0.75 [a]	0.1 μM ~ 12 μM	0.098 μM	Raoof et al., 2009
NHPDA/FePt/CNT [Ml]	CV	7.0	0.41 [a]	4 nM ~ 340 μM	1 nM	Karimi-Maleh et al., 2014
Ethynylferrocene–NiO/ MWCNT [Ml]	CV	6.0	0.48 [a]	0.01 μM ~ 200 μM	6 nM	Shahmiria et al., 2013
benzamide derivative-MWCNT [Ml]	SWV	7.0	0.29 [a]	0.09 μM ~ 300 μM	0.05 μM	Ensafia et al., 2013
CoPc immobilized on nitrogen-doped graphene [Ml]	AMP	13	-0.05 [c]	1 μM ~ 8 mM	1 μM	Xu et al., 2015
Au nanoparticles [Ml]	DPV	7.4	0.33 [a]	20 μM ~ 200 μM	0.082 μM	Atta et al., 2012
CNT–ionic liquid–epinephrine [Ml]	DPV	7.0	0.28 [c]	0.1 μM ~ 30 μM	0.04 μM	Liu et al., 2015
FeT4MpyP-MWCNT [Ml]	~	7.4	0 [a]	5 μM ~ 5 mM	0.5 μM	Luz et al., 2008
FTO [Ml]	LSV	4.4	0.27 [c]	~	~	Mu and Yang, 2016
Pt-NiCo [Ml]	AMP	7.4	0 [a]	0.1 μM ~ 645 μM	0.02 μM	Zhang et al., 2010
TCNQ/GO/GCE [Ml]	AMP	7.2	-0.05 [a]	0.25 μM ~ 124.3 μM [1]	0.15 μM [1]	This work

			0.1 [a] 0.5 [a]	124.3 μM~1.67 mM [1] 0.25 μM ~ 174.3 μM [2] 174.3 μM-1.18 mM [2]	0.1 μM [2]	
I^-/I_2 [Mr]	CV	~	0.95 [c]	19.9 μM ~ 629.4 μM;	21.28 μM	Valero-Ruiz et al., 2016
4-methylesculetin–boric acid [Mr]	CV	8.0	0.22 [a]	~	~	Salehzadeh and Nematollahi, 2013
Pyrroloquinoline Quinone [Mr]	AMP	3.5	0.50 [a]	~	13.2 μM	Inoue and Kirchhoff, 2000
4,4'-biphenol [Mr]	CV	7.0	0.35 [a]	~	~	Shayani-Jam and Nematollahi, 2011b
Acetaminophen [Mr]	CV	7.0	0.45 [a]	~	~	Shayani-Jam and Nematollahi, 2010a
Rutin [Mr]	DPV	7.0	0.27 [a]	0.5 μM ~ 25 μM	0.08 μM	Huang et al., 2015
Catechol [Mr]	CV	7.0	0.40 [b]	10 μM ~ 60 μM	3.0 μM	Lee et al., 2015
Catechol [Mr]	CV	7.4	-0.16 [a]	1 μM ~ 500 μM	0.5 μM	Zhao et al., 2016
$[IrCl_6]^{2-}$ [Mr]	CV	7.0	0.72 [a]	~	~	Medina-Ramos et al., 2013
Catechol derivatives [Mr]	CV	7.3	0.25	~	~	Pacsial-Ong et

						al., 2006

Where Ml = material; Mr = mediator; OP = oxidation potential; a = vs. Ag/AgCl electrode; b = vs. Ag electrode; c = vs. Saturated Calomel Electrode; AMP = Amperometric; NHPDA = N-(4-hydroxyphenyl)-3,5-dinitrobenzamide; DPV = Differential Pulse Voltammetry; LSV = Linear Sweep Voltammetry; SWV = Square Wave Voltammetry; AMP-CE = Amperometric method coupled with capillary electrophoresis; SPE = screen-printed electrode; MPT-HP-β-CD = 2-Hydroxypropyl-β-Cyclodextrin enveloped 10-methylphenothiazine; FeT4MpyP = iron(III) tetra-(N-methyl-4-pyridyl)-porphyrin; FTO = fluorine doped tin oxide; ITO = indium tin oxide; CoPcTF = Cobalt phthalocyaninetetrasulfonate; CNT = carbon nanotube; MWCNT = multiwall carbon nanotube; NiHCF = nickel hexacyanoferrate; [1], obtained at 0 V; [2], obtained at 0.1 V.

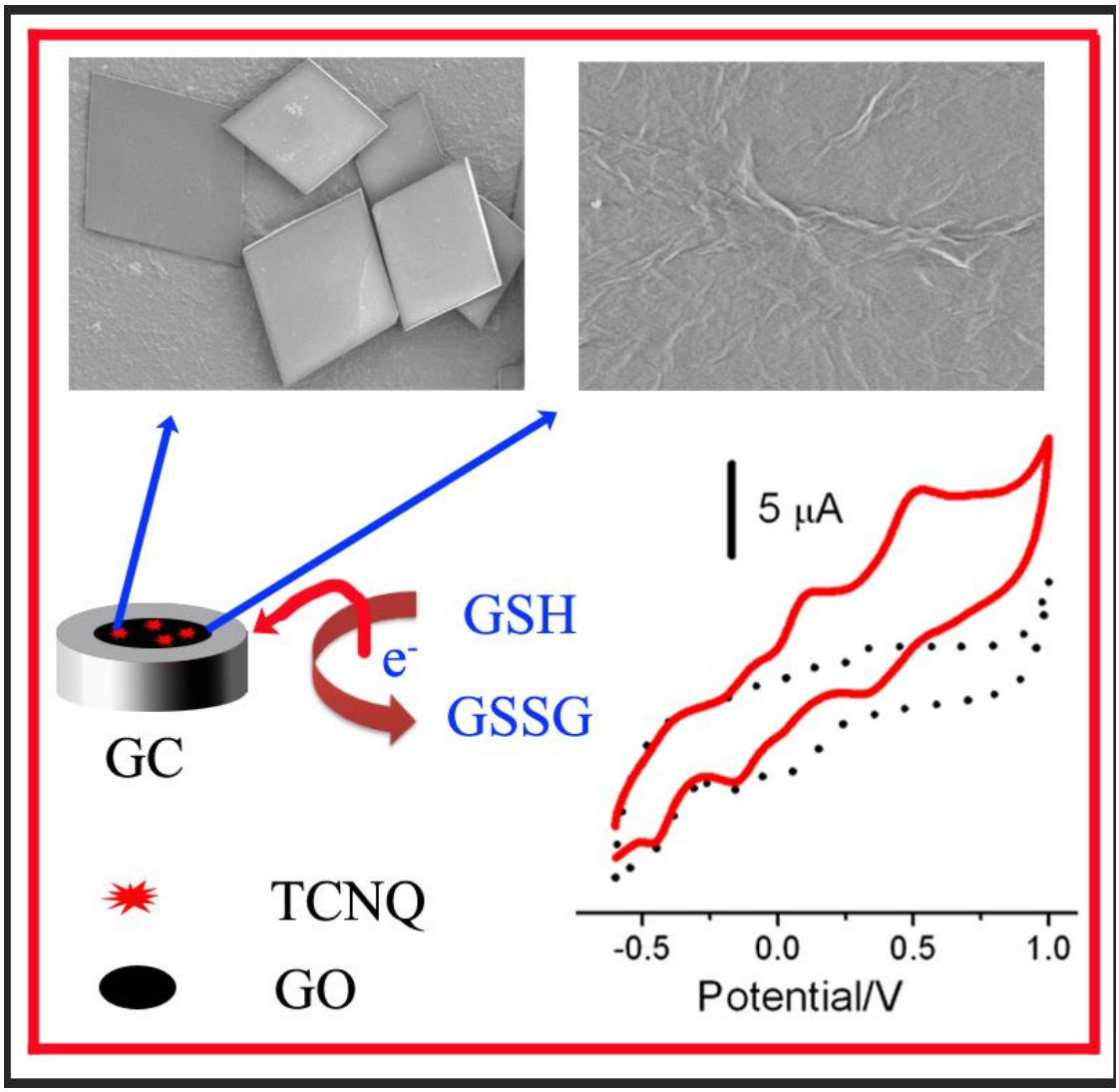

Graphical Abstract: TCNQ and GO modified GCE for the electrocatalytic oxidation of GSH